INL/RPT-24-80762

Advanced Reactor Technologies

Interim Development of New Class B Code Case with Variable Design Lifetime and Enhanced Design Rules to Guard Against Cyclic Structural-Failure Mode

SEPTEMBER 2024

Heramb Mahajan

Idaho National Laboratory

Robert Jetter

JFoster & Associates LLC

Yanli Wang

Oak Ridge National Laboratory

Idaho National Laboratory

Battelle Energy Alliance manages INL for the U.S. Department of Energy's Office of Nuclear Energy

INL/RPT-24-80762

Interim Development of New Class B Code Case with Variable Design Lifetime and Enhanced Design Rules to Guard Against Cyclic Structural-Failure Mode

Heramb Mahajan
Idaho National Laboratory
Robert Jetter
JFoster & Associates LLC
Yanli Wang
Oak Ridge National Laboratory

September 2024

Idaho National Laboratory
Advanced Reactor Technologies
Idaho Falls, Idaho 83415

http://www.inl.gov

Prepared for the
U.S. Department of Energy
Office of Nuclear Energy
Under DOE Idaho Operations Office
Contract DE-AC07-05ID14517

Page intentionally left blank

INL ART Program

Interim Development of New Class B Code Case with Variable Design Lifetime and Enhanced Design Rules to Guard Against Cyclic Structural-Failure Mode

INL/RPT-24-80762

September 2024

Technical Reviewer: (Confirmation of mathematical accuracy, and correctness of data and appropriateness of assumptions.)

Michaed D. McMurtrey ART GCR High Temperature Alloys Lead	9/9/2024 Date
Michael E. Davenport ART Project Manager	9/4/2024 Date
Michelle T. Sharp INL Quality Assurance	9/4/2024 Date

SUMMARY

This report provides an update on the ongoing development of the new American Society of Mechanical Engineers Boiler and Pressure Vessel Code (BPVC), Section III, Division 5, Class B rules to address the potential structural failure modes of Class B components. An initial design-by-analysis approach and supporting design rules are presented. The elastic-perfectly plastic analysis approach has been adopted for primary load limit and ratcheting check to prevent component failure against the structural failure mode against primary load and strain accumulation due to cyclic loads. The creep-fatigue (CF) damage assessment uses explicitly defined elastic follow-up, calculated from the stress-concentration region of a given component. Damage-fraction calculation uses a novel coupled approach to capture the influence of the elastic follow-up. The proposed Class B rules do not use the stress-classification approach, but use the combined loads in the component design process.

Page intentionally left blank

ACKNOWLEDGMENTS

This research was sponsored by the U.S. Department of Energy (DOE) under Contract No. DE-AC07-05ID14517 with Idaho National Laboratory (INL), which is managed and operated by Battelle Energy Alliance, and under Contract No. DE-AC05-00OR22725 with Oak Ridge National Laboratory, which is managed and operated by UT-Battelle LLC.

Programmatic direction was provided by the Office of Nuclear Reactor Deployment of the DOE Office of Nuclear Energy. The authors gratefully acknowledge the support provided by Sue Lesica of DOE-NE, federal materials lead for the Advanced Reactor Technologies (ART) Program; Matthew Hahn of DOE-NE, federal program manager of the ART Gas-Cooled Reactors Campaign; and Gerhard Strydom of INL, ART Gas-Cooled Reactors national technical director. Authors gratefully acknowledge Ting-Leung Sham of the U.S. Nuclear Regulatory Commission (NRC), who served as the Advanced Materials Technology Area Lead for the ART Program within DOE-NE prior to joining the US-NRC, for his technical guidance towards code-case development.

The authors would like to acknowledge Derrick Peace of Becht for reviewing the code case and providing insightful recommendations.

Page intentionally left blank

CONTENTS

FIGURES

TABLES

Page intentionally left blank

ACRONYMS

ART	Advanced Reactor Technologies (Program)
ASME	American Society of Mechanical Engineers
BPVC	Boiler and Pressure Vessel Code
CF	Creep-fatigue
CH	Compressive hold
DBA	Design by analysis
DOE	Department of Energy
EPP	Elastic-Perfectly Plastic
FEA	Finite Element Analysis
HBA	Subsection HB, Subpart A
HBB	Subsection HB, Subpart B
HCA	Subsection HC, Subpart A
HCB	Subsection HC, Subpart B
ID	Inside dimensions
ISSC	Isochronous Stress Strain Curves
NE	Office of Nuclear Energy
p-SBSMT	Pressurized Single Bar Simplified Model Test
p-SMT	Pressurized Simplified Model Test
SBSMT	Single Bar Simplified Model Test
SMT	Simplified Model Test
SSC	Structures, systems, and components

Interim Development of New Class B Code Case with Variable Design Lifetime and Enhanced Design Rules to Guard Against Cyclic Structural-Failure Mode

1. INTRODUCTION

Generation IV nuclear reactors, which include gas-cooled reactors, molten-salt reactors, and sodium-cooled fast reactors, are expected to operate in the temperature range of 400–800°C, with a design life up to 60 years. Prolonged exposure to elevated temperatures for long time periods makes components susceptible to such time- and temperature-dependent failure modes due to sustained operational load, strain accumulation, and ratcheting due to cyclic loads and creep-fatigue (CF) damage accumulation. Component-construction rules address these failure modes and provide reasonable component-integrity assurance without excessive conservatism.

American Society of Mechanical Engineers (ASME) Boiler and Pressure Vessel Code (BPVC), Section III, Division 5 provides construction rules for vessels, piping, supports, core support structures, valves, and pumps operating at wide temperature ranges [1]. The United States Nuclear Regulatory Commission issued a draft interim staff guidance on the acceptability of 2017 Edition of ASME BPVC, Section III, Division 5 for structures, systems, and components (SSCs) design of high-temperature reactors [2].

Section III, Division 5 is organized by code classes based on defined operational purpose, anticipated failure modes, and SSCs safety assurance. The structure of Section III, Division 5 for metallic SSCs is presented in Table 1. The metallic SSC applications cover general design requirements, coolant boundaries, metallic supports, and core-support SSCs. Safety-related SSCs, performing safety-significant functions, are classified under Class A, and subsequent Section III, Division 5 subsections for coolant boundary vessel are HBA, and HBB. Class B covers non-safety-related SSCs performing safety-significant functions, and subsections HCA and HCB cover vessel-construction rules. Core support structures for low and high temperature service is covered under HGA and HGB, respectively.

Table 1. Organization of classes for metallic materials in Section III, Division 5.

SSC Applications	Service Temperature	Section III Division 5 Subsections		
		Class A	Class B	Class SM
General requirements	Low temperature service	HAA	HAA	HAA
Coolant boundary vessel	Low temperature service	HBA	HCA	–
	High temperature service	HBB	HCB	–
Metallic supports	Low temperature service	HFA	HFA	–
Core support	Low temperature service	–	–	HGA
	High temperature service	–	–	HGB

Existing Class B rules use material allowable stresses, defined under Section II, Part D, Tables 1 and 2 [3]. For high-temperature service (HCB), allowable stresses are calculated by extrapolating the temperature-dependent creep data to 100,000 hours. Although the allowable stress values are based on creep properties at 100,000 hours, there are no restrictions on the service life. Class B rules provide an efficient approach for design by rule (DBR) calculations for primary loads. However, for cyclic loads at elevated temperatures, the Class B methodology does not consider cyclic loading due to thermal and loading transients. Thus, vessels constructed according to the existing Class B rules would be vulnerable to the CF failure mode. Piping components have limited CF damage-fraction calculations, which typically lead to highly conservative designs. Creep-fatigue damage assessment for other SSCs is not covered in the existing Class B methodology.

Current Generation IV nuclear reactors are expected to be constructed with SSCs operating in the creep regime under cyclic loads. Such operations result in several SSCs classified as Class B SSCs which fall under HCB in Section III, Division 5. Due to the limitations of current Class B methodology, reactor certificate holders are forced to treat Class B SSCs as Class A. This treatment leads to two effects: (1) conservative selection of the design margin on operating life and cyclic failure modes of SSCs which results in a conservative design, and (2) limited material selection for SSCs construction, as Class A methodology allows the use of only six materials. Addition of new materials under the Class A material list require a vast material database. Current Class B allows a wide set of materials, but there is need for an approach to extrapolate the existing data beyond 100,000 hours. Although the design by analysis (DBA) approach of Class A may be attractive due to efficiency in addressing cyclic failure modes, Class A DBA may be too restrictive with limited materials selections for Class B applications. Thus, a new DBA for Class B components is needed which provides integrity assurance with less restrictions, more material selections and minimal additional test requirements. An additional goal is to avoid the tedious process of stress classification.

To address these gaps and limitations, a new variable design life, Class B code case, was proposed [4]. Past work has laid a foundation for Class B code-case development, as documented in [4,5]. This report presents the ongoing work towards Class B code-case development. The proposed design methodology is evaluated against test-failure data and sample problems to establish conservatism against different failure modes. Sample problems were selected to assess the design rules. Material-data requirements are documented for new-material additions to support time- and temperature-dependent design.

2. PROPOSED CLASS B DESIGN METHODOLOGY

This section presents the overview of proposed Class B methodology to address potential failure modes at elevated temperature listed as failure under primary loads, strain accumulation due to ratcheting, and failure due to cyclic loads at elevated temperature, dominated by CF damage accumulation. The proposed DBA rules adopt use of the elastic-perfectly plastic (EPP) methodology through finite element analysis (FEA). Figure 1 presents the flow chart of EPP FEA for the selected evaluation approach.

The EPP FEA process flow starts with detailed component geometry, identified component loads, and support-boundary conditions to build a finite-element model. The EPP FEA method uses small strain computation and appropriate finite-element discretization to model all the component details. An isotropic, temperature-dependent EPP material model is defined using temperature-dependent elastic-material properties and yield stresses. The yield stresses in the EPP model are replaced by pseudo-yield stresses, where pseudo-yield stress is a time- and temperature-dependent stress. . The subsections below discuss pseudo-yield stress-evaluation approaches to address specific failure modes. The pseudo-yield stress captures time- and temperature-dependent material properties at the elevated-temperature material response for the desired life. Using this material pseudo-yield stress definition and finite-element model, EPP FEA is performed, and the solution is used to assess the component response against design criteria for each selected evaluation approach. In this report, steps highlighted in green color are referred as EPP FEA, and steps in blue are referred as the pseudo-yield stress-determination approach.

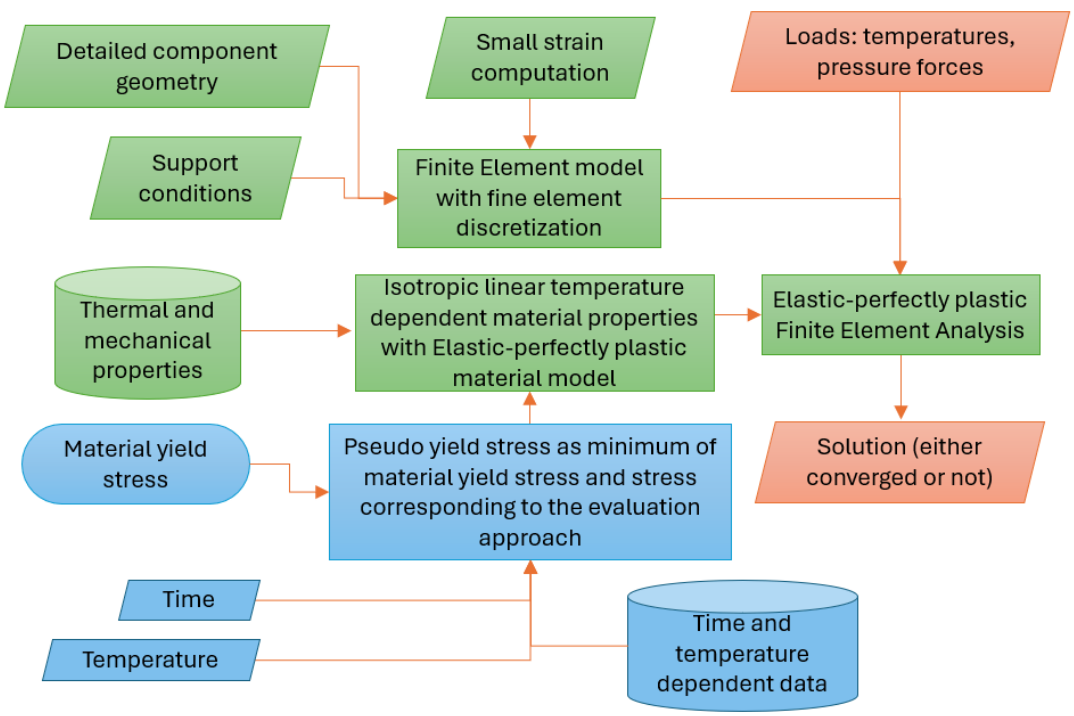

Figure 1. Flow chart of the EPP FEA approach.

2.1. Primary Load Limit

The evaluation procedure for load-controlled stress serves two purposes: (1) it explicitly accounts for long-term specific design life, and (2) it avoids stress classification. Design methodology under the primary load limit provides component-integrity assurance under sustained loads during steady-state operation. The goal of the primary load limit check is to evaluate the use fraction for different load cycles. The framework of Class A Code Case N-924 is used as basis to develop the Class B primary limit check, as shown in Figure 2 [6].

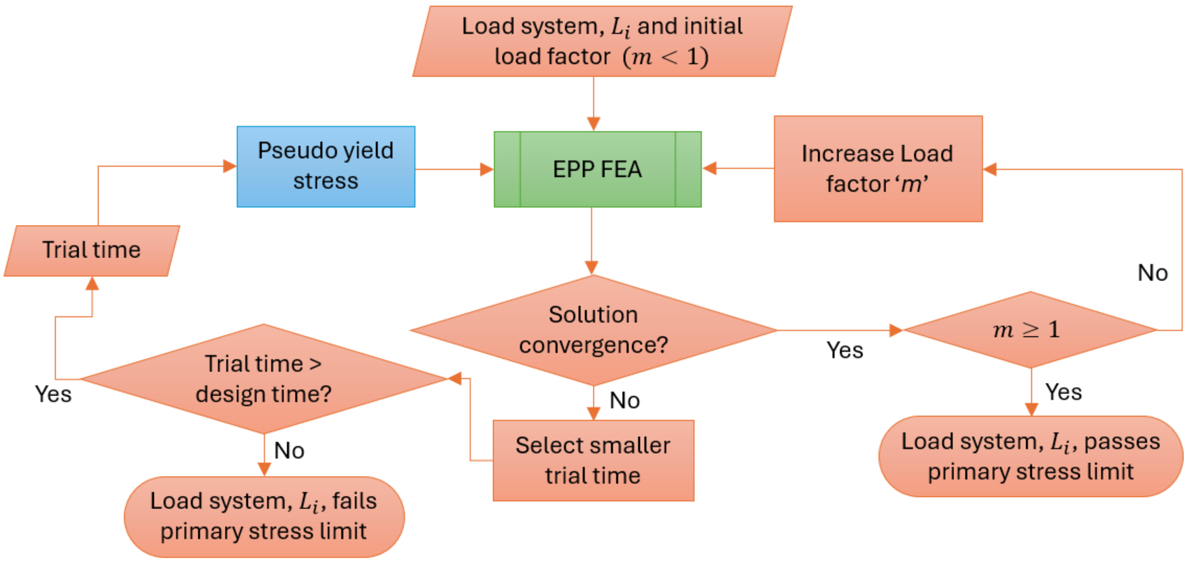

Figure 2. Flow chart of the primary load limit evaluation.

The allowable design loading is based on either of the following: design-by-analysis (DBA) procedures in NCD-3300, 3400, and 3500, or on the limit load in CC N-924 EPP FEA DBA procedures. For service loadings, EPP FEA DBA procedures in CC N-924 are applicable. The proposed primary-limit procedure avoids stress classification. Steady-state temperatures during load cycle and trial time greater than the design time are selected as inputs for pseudo yield stress. Pseudo yield stress is defined as stress corresponding to the selected trial time and temperature from the time- and temperature-dependent allowable stress. The pseudo-yield stress replaces the yield stress of the material model, and the factored steady-state load system is applied to the EPP FEA by multiplying a load factor, m, to loads. If the factored load with selected load factor $(m < 1)$ achieve solution convergence, the load factor is increased, and an increased load is applied in EPP FEA. These steps are repeated until the load factor reaches a value of one. Solution convergence observed at the load-factor value of one suggests stresses due to applied loads are smaller relative to the pseudo-yield stress of the material. In other words, plastic collapse is not observed. The use fraction is calculated as a ratio of design time of selected load cycle to the selected trial time. If summation of use fractions from all load cycles is less than or equal to one, then the component passes the primary load limit.

If solution convergence is not observed at or below a load factor equal to one, plastic collapse occurred in the component, and the selected trial time fails the primary-stress limit. A new trial time is selected, which is smaller than the previous trial time. If the new trial time is greater than the design time of a given load system, a new pseudo-yield stress corresponding to the new trial time is calculated, and all steps are repeated. If the trial time fails to satisfy the primary-stress limit and trial-time reach value of design time, then the selected load system fails the primary-stress limit check.

2.2. Ratcheting Check

The ratcheting check evaluates component for strain accumulation. Code Case N-861-2 provides strain limit evaluation for Class A components [6]. A similar methodology was adopted to develop code rules for ratcheting check for Class B (Figure 3). The proposed ratcheting check for Class B SSCs approach is shown in Figure 3. Unlike Class A EPP approach, the proposed method uses a fixed inelastic strain value of 0.01 for base metal and 0.005 for weldments as input to calculate the pseudo yield stresses. Using operation cycle time, temperature and inelastic strain of 0.01, pseudo yield stresses are calculated using the material yield stress and isochronous stress strain curves (ISSCs) of material at given temperature and time. This step results in a spatial distribution of time and temperature dependent pseudo yield stress definition. These pseudo yield stresses replace the material yield stress in the EPP material model. A composite load cycle history based on the Design Specifications is defined and applied on the component model and the EPP FEA procedure is used. Strain histories at all points from the EPP FEA are checked for shakedown. If shakedown is observed, selected components and loads pass the ratcheting check. If shakedown is not observed, the selected composite load cycle fails the strain limit evaluation. In this case, a revision of composite load cycle or change in component geometry may be needed.

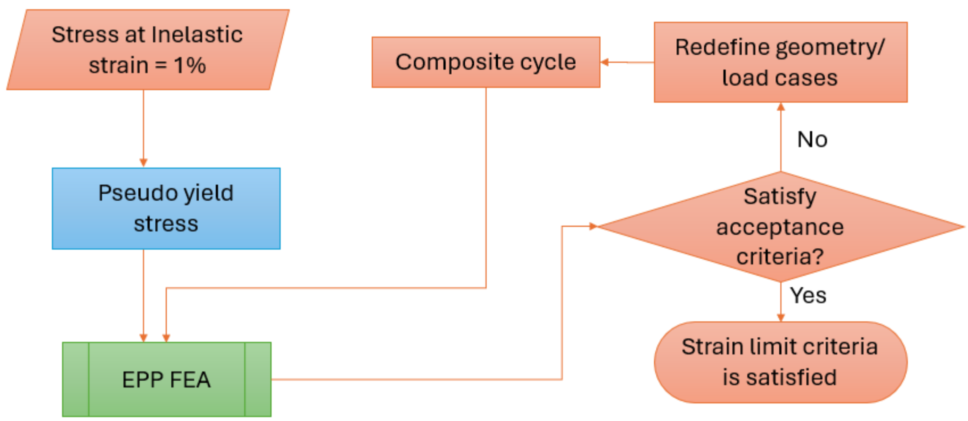

Figure 3. Flow chart of the ratcheting check.

2.3. Creep-Fatigue Damage Assessment

This subsection discusses rules to address component failures due to CF damage governed by cyclic loads at elevated temperatures. Figure 4 provides a flow chart of the proposed CF assessment.

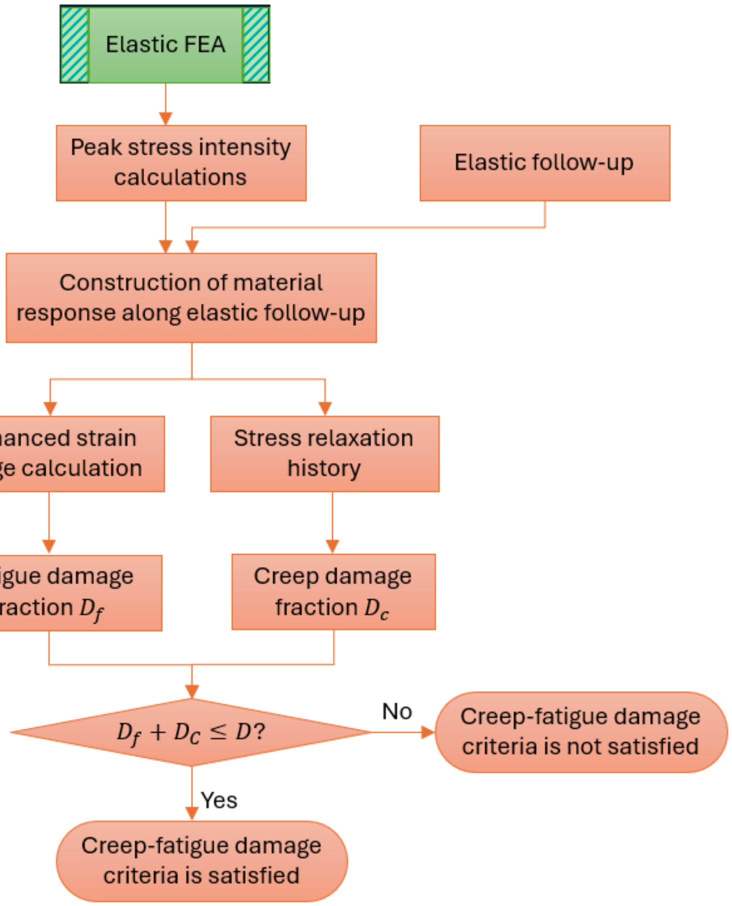

Figure 4. Flow chart of the creep-fatigue damage assessment.

A CF damage assessment starts with the elastic FEA. This analysis is identical to the EPP FEA, except elastic analysis uses only elastic-material model properties. Geometric modeling steps, small strain computation, boundary conditions, and elastic temperature-dependent material properties are defined for elastic FEA as they are for EPP FEA. Each load system is individually applied, and stress histories from all integration points for each load system are used to calculate the alternating peak stress intensity, as defined in Section III, Appendix XIII-2400 [7].

Elastic-stress concentration factor, K_e, for a component is calculated as a ratio of total stress to linearized stress from elastic analysis. An elastic follow-up is calculated as a function of stress concentration factor using Equation (1).

$$q = \max \begin{cases} 1.5K_e \\ 2 \end{cases} \quad (1)$$

The maximum alternating peak stress intensity for given load system and elastic follow-up are used with ISSCs of the materials to construct a stress time history and stress-strain response. This step has been discussed in detailed in the previous work and is summarized graphically in Figure 5 [5]. Peak stress intensity is plotted at Point O, and a line is constructed passing through Point O and having slope $-\frac{E}{q-1}$, where E is the elastic modulus. The stress-relaxation history is bounded by the lower bound stress, which is defined as the pseudo-yield stress at the longest trial time, which approaches the collapse load in the component. This lower-bound stress adopts the EPP FEA approach as does the primary-stress-limit check, and it uses a factored load system. One of the methods to calculate the lower bound stress is presented in Figure 4. Using an arbitrarily chosen pseudo-yield stress, EPP FEA is conducted and checked for plastic collapse, with a load factor of m. If plastic collapse is not observed, m is increased, and these steps are repeated until plastic collapse is observed. Critical load factor, m^* is defined as the maximum load factor at which the solution converged where plastic collapse is not observed. The lower-bound stress is defined as a ratio of an arbitrarily chosen pseudo-yield stress to the critical load factor, m^*.

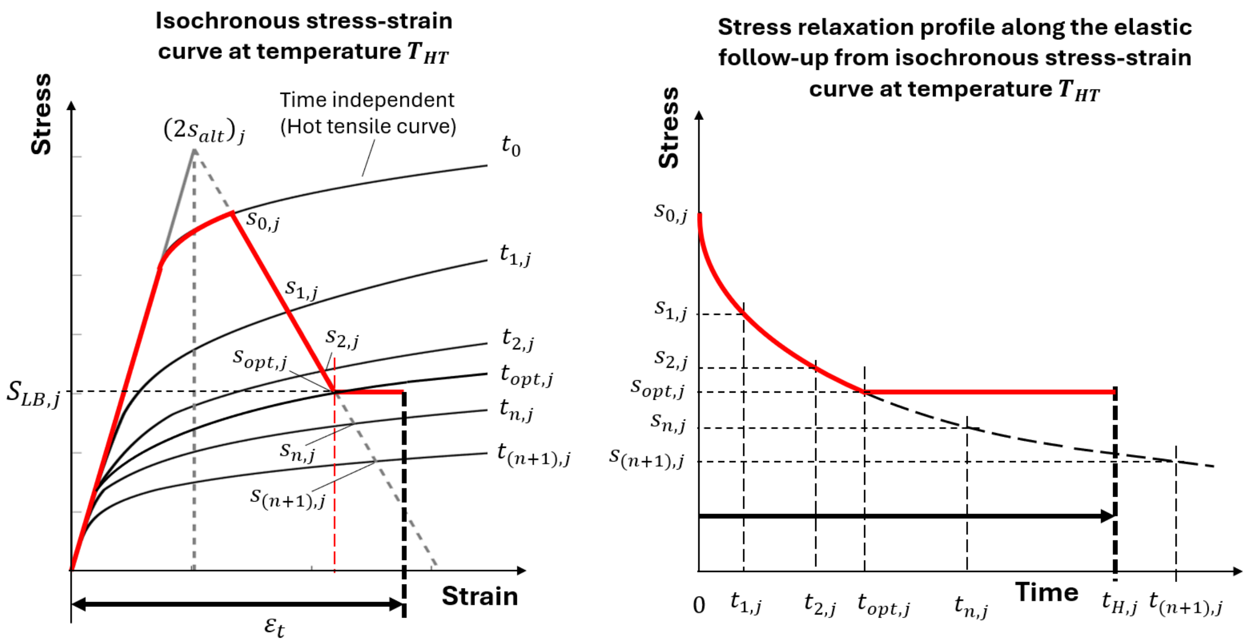

Figure 5. Construction of stress-strain path on ISSCs showing steps to determine stress-relaxation history for creep-damage fraction and enhanced strain-range determination for fatigue-damage calculation.

The enhanced strain range at the end of dwell time is calculated using strain equation as shown in Equation (2) explicitly accounts the influence of elastic follow-up and lower bound stress. It is calculated based on the strain history. Fatigue design curves at the given temperature are used to determine cycles to failure for calculated enhanced strain range, and the subsequent fatigue damage fraction is calculated. Equation (3) is used to calculate the stress-relaxation history. This stress history, bounded by a lower bound stress, is used to calculate the creep-damage fraction using minimum stress to rupture material data. An example of stress versus time history of one cycle is shown in the red curves in Figure 5. For given cycle type j, stresses $s_{i,j}$ corresponding to the time $t_{i,j}$ are calculated, where i is total amount of time steps. This stress history is bounded by the lower bound stress S_{LB}. Creep damage accumulated in one cycle is calculated and multiplied with design cycles to calculate the total creep damage fraction. The fatigue and creep-damage fractions are calculated using Equations (4) and (5), respectively. These damage fractions are compared against the CF damage envelope. If damage fractions are in the acceptable region of the damage envelop, as shown in Figure 6, selected component and load systems pass CF damage assessment.

$$\varepsilon_t = \frac{q}{E}\sigma_{peak} - \frac{q-1}{E}\sigma_j + \langle t_{dwell} - t_j \rangle \times \rho_s(S_{LB}) \quad (2)$$

$$t = \frac{q}{E}\frac{\sigma_{peak}-\sigma}{\dot{\varepsilon}(\sigma)} - \frac{\varepsilon_{plastic}(\sigma)}{\dot{\varepsilon}(\sigma)} \quad (3)$$

$$D_f = \sum_j \frac{n}{N_d} \quad (4)$$

$$D_c = \sum_j n \left(\int_0^{t_h} \frac{dt}{T_d(\sigma,T,t)}\right) \quad (5)$$

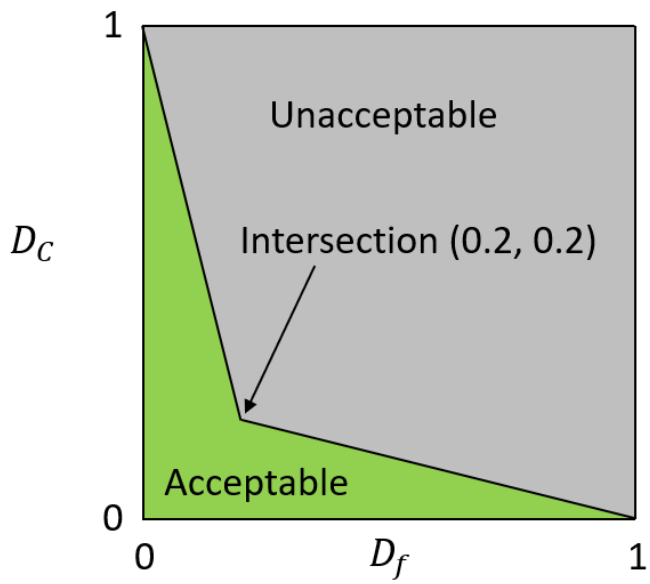

Figure 6. Creep-fatigue damage envelop.

3. EVALUATION OF DESIGN BY ANALYSIS RULES

The proposed Class B methodology is evaluated against the Section III, Division 5, Class A analysis methods. Although these design methods are based on different assumptions and are different from each other, the goal is to evaluate the conservatism and ease of the proposed Class B DBA approach. The Class A inelastic-analysis approach uses detailed component geometry with viscoplastic-material modeling per Appendix Z in Section III, Division 5 [1]. Material-model parameters were determined using a vast set of test data that predicts cyclic hardening, softening, creep rates, and coupled CF interaction of materials [8]. Thus, viscoplastic constitutive models in Appendix Z can capture the complex CF material response. Using the viscoplastic constitutive-material model and detailed component geometry, stress-strain time history is obtained at all points in a component. Using these data and a strain-range determination per HBB-T-1413, the fatigue damage fraction is calculated. While calculating creep-damage fractions per equation HBB-T-1411 (10), stresses are divided by a safety factor, K', amplifying stresses to calculate time to rupture, T_d. For inelastic analysis, factor K' takes a value of 0.67, per Table HBB-T-1411-1, which increases stress intensities by 1.5 times. This step introduces conservative estimates of the creep damage in inelastic analysis. This analysis methodology is referred in this report as "Class A inelastic."

In this report, a separate evaluation approach was conducted using stress-strain time histories from full inelastic analyses. Strain-range determination and subsequent fatigue-damage calculation were identical to the Class A inelastic-analysis method; however, factor K' was selected for creep-damage calculation, indicating no additional conservatism in the creep-damage calculations. This approach is referred in this report as "inelastic," which minimizes the conservatism while estimating the maximum design life. The following subsections provides evaluation of the proposed rules against test failure data and sample problems with inelastic analyses. The maximum design life, N_{max}, is calculated for each test and sample problems using Equations (6) and (7).

$$N_{max} = \frac{1}{dD_f\left[m + \frac{1-a_c}{a_c}\right]}, \quad \text{for } m > \frac{a_f}{a_c} \tag{6}$$

$$N_{max} = \frac{1}{dD_f\left[m\frac{1-a_f}{a_f} + 1\right]}, \quad \text{for } m < \frac{a_f}{a_c} \tag{7}$$

Where, m is the ratio of creep damage fraction dD_c and fatigue damage fraction dD_f accumulated in one cycle; (a_f, a_c) are coordinates of the damage envelop intersection point. The creep and fatigue damage fractions accumulated in one cycle are calculated using proposed Class B analysis and maximum design life is calculated. This maximum design life is compared against either test failure data or maximum design life from inelastic method to evaluate the conservatism in the proposed Class B methodology.

3.1. Evaluation of Rules Against Experimental Data

Two specimen geometries from literature were selected as candidates to evaluate the proposed DBA rules. Test failure cycles were compared against maximum design cycles calculated from ratcheting check and CF assessments. Maximum design cycles for the ratcheting check are calculated by selecting a trial design time, which is set to the time to reach failure cycles, calculating corresponding pseudo-yield stress, and conducting EPP FEA as discussed in the previous section. The trial time is revised until shakedown is observed. Maximum design cycles from CF assessment are determined by calculating a creep- and fatigue-damage fraction due to one cycle, and iterating a number of cycles to reach the total damage to satisfy the damage envelope check. The following subsection presents a detailed comparison of the proposed DBA rules against the test failure data.

3.1.1. Pressurized Single-Bar Simplified-Model Test (p-SBSMT)

The first geometry consists of a tubular specimen, fabricated from A617 material, as shown in Figure 7. This specimen is referred as pressurized single bar simplified model test (p-SBSMT) specimen, which was developed and documented in [9–13]. The purpose of these tests was to investigate the material response at elevated temperature when subjected to representative component loads. These tests provide cycles to failure for internal pressure and elastic follow-up loads capturing the key component characteristics. Thus, cycles to failure from the p-SBSMT geometry with pressure and elastic follow-up were used in this report to evaluate the conservatism in the Class B methodology. The internal volume is pressurized, and cyclic displacements are applied at the specimen end. Strain rate is measured in the gauge section of specimen, and end displacement is controlled through software to induce the predetermined elastic follow-up in the gauge section. The detailed test setup, apparatus, and procedure is discussed in literature [9,10].

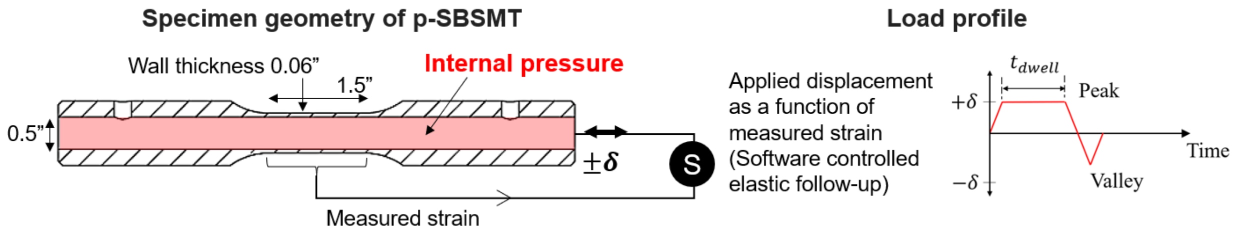

Figure 7. Test specimen geometry and load profiles of p-SBSMT test specimen [9,10,11,13].

The load parameters are selected to cover different pressure, elastic follow-up and strain ranges. Maximum design cycles for each load case are calculated using the proposed DBA Class B procedure and compared against the test failure cycles, N_f, in Table 2.

Table 2. Test parameters for p-SBSMT, and comparison of failure cycles from tests against the maximum design cycles from the proposed Class B approach. TH: tensile hold.

ID	P (MPa)	q	$\Delta\varepsilon$ (%)	TH (sec)	Test data N_f	N_{max}* Class B CF*	Primary Limit check evaluated at 1000 hours	Ratcheting Check, Maximum design cycles
SBAP 4	0.01	6.1	0.18	600	3641	43	Pass	Pass, 3
SBAP 5	1.03	3.4	0.53		201	10	Pass	Fail, 0
SBAP 6	0.01	3.53	0.53		347	11	Pass	Fail, 0
SBAP 9	1.03	1.96	0.28		996	85	Pass	Pass, 1
SBAP 7	0.01	2.02	0.25		3224	104	Pass	Pass, 3

*N_{max} CF Maximum design cycles calculated from creep-fatigue assessment.

For the primary-limit check, S_{mt} values at trial time of 1000 hours are defined as the pseudo-yield stress. To satisfy the primary limit stress check, the use fraction needs to be smaller than one. This condition suggest that the trial time needs to be greater than the time to failure from tests. Thus, the time of 1000 hours is selected as trial time for all cases. The primary limit-check process flow shown in the previous section was used. Pressure loads were identified as loads during steady-state operation. All cases passed the primary limit-check criterion, suggesting specimen-geometry safety against sustained loads for 1000 hours, which was longer than the actual failure cycle time during cyclic loads.

The ratcheting-check methodology, discussed in the previous section, was adopted with pseudo-yield stress defined at 0.01 of inelastic strain at test temperature and trial time, t_{trial}. A trial design time was selected as the time to reach the failure cycle for each case, and EPP FEA was conducted. If plastic collapse or ratcheting was detected, t_{trial} was reduced, and a new pseudo-yield stress was calculated to conduct EPP FEA. This loop was repeated until a t_{trial} showed no indication of ratcheting, and that time was used to calculate the allowable maximum design cycles based on the ratcheting check. The last column in Table 2 shows the ratcheting check criteria and the maximum design cycles for which ratcheting criteria passed. The maximum design cycle is determined from the trial time for which no ratcheting is detected in the EPP FEA results. As shown in Table 2, the ratcheting check yielded significantly lower design cycles for all cases and failed for all trial times for specimens with large strain ranges. Because this specimen geometry had a uniform cross-section with large cyclic displacements applied on the specimen end, large deformation resulted in plastic collapse due to yielding of all points across thickness. The maximum design lives estimate, N_{max}, from proposed Class B were conservative when compared against test failure cycles N_f. The Class B methodology adopted the elastic follow-up calculation based on stress concentration factor. The p-SBSMT geometry was smooth, which resulted as the minimum elastic follow-up value of 2. The maximum design cycle estimate using this minimum elastic follow-up yielded conservative estimates compared to the test failure data with elastic follow-up greater than two. This comparison shows that the minimum elastic follow-up of 2 conservatively bounds the design life estimates for all cases when stress concentration factor is not controlling.

3.1.2. Pressurized Simplified Model Test (p-SMT)

The second geometry consists of simplified model test (SMT) specimen fabricated from A617 material, as shown in Figure 8, which was developed and documented in [11–13]. The internal volume is pressurized, and cyclic displacements are applied at the specimen end. The two cylinders in series interact during displacement dwell and induce predetermined elastic follow up. The detailed test-setup, apparatus and procedure are discussed in literature [11–13]. The test parameters, cycles to failure, and results from the DBA rules comparison are presented in Table 3. All specimens had tensile hold of 600 seconds at peak displacement, and few had a compressive displacement hold, as listed in Table 3.

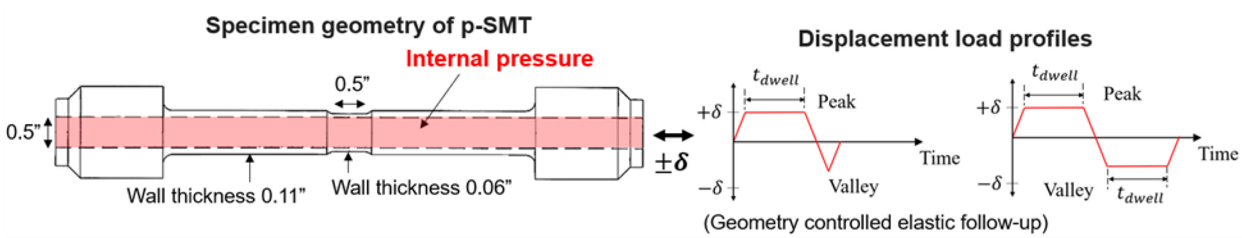

Figure 8. Test specimen geometry and load profiles of pressurized simplified model test (p-SMT) test specimen [11–13].

Table 3. Test parameters for p-SMT, and comparison of failure cycles from tests against the maximum design cycles from proposed Class B approach. CH: compressive hold.

ID	T (°C)	P (MPa)	δ (mm)	CH (sec)	N_f	N_{max} from CF assessment			Primary Limit Check
						Class A Inelastic K'=0.67	Inelastic K'= 1	Class B	
P01	950	0.01	0.114	0	220	1	25	12	Passed
P02	959	1.39	0.114	0	220	1	60	12	Passed
P04	957	3.45	0.114	0	200	1	35	12	Passed
P03	958	5.17	0.114	0	150	1	36	12	Passed
P06	950	5.17	0.114	0	140	1	21	12	Passed
P09	953	5.17	0.076	0	320	5	93	25	Passed
P12	950	0.01	0.0635	0	1360	11	119	38	Passed
P13	950	1.05	0.0635	0	820	11	122	38	Passed
P14	850	2.76	0.0762	0	3440	26	274	134	Passed
P15	850	0.01	0.0762	0	3460	25	265	134	Passed
P05	950	0.01	0.114	600	320	1	6	10	Passed
P08	950	3.76	0.114	600	280	1	5	10	Passed
P07	950	5.17	0.114	600	180	1	5	10	78*

*Primary limit check failed; optimum cycle is calculated from the trial time at which primary limit check passed.

The first comparison is between cycles to failure from tests, N_f, and the maximum allowable design life from Class B CF methodology. This comparison shows that the proposed Class B methodology is conservative compared to the test failure data. As stresses due to cyclic loads are significantly higher than the stresses due to pressure, stress intensity calculations per Section III, Appendix XIII-2400 are governed by cyclic loads. Load cases P01–P04, and P06 have same displacement profile and influence on peak-stress intensities because pressure is low. This resultant peak-stress intensity for these cases is the same, which results in a similar estimate of Class B maximum design life. For load cases P05, P07, and P08, peak-stress intensity was same as the P01 case; however, total cycle time was longer due to a CH that resulted in smaller cycle estimates. Experimental values of elastic follow-up in load cases at 950°C ranged from 3.5 to 4.1. The stress-concentration factor for p-SMT geometry was 1.37; thus, the minimum elastic follow-up of 2 was used for all cases.

The second comparison is between cycles to failure from tests, N_f, and maximum cycles from Class A inelastic, with K' value of 0.67 and inelastic analysis with K' of one. As expected, inelastic analysis with K' of one yielded larger design cycles. Due to a knock-down factor on stresses, Class A inelastic-analysis procedure estimates significantly lower design cycles relative to failure cycles from tests. The minimum stress-to-rupture tables are developed from a lower bound calculated from the 1.65 times standard error of estimate of data, meaning 95% of data will be larger than the data table. This introduces conservatism on the material-rupture properties, which is observed while comparing design life with inelastic analysis with K' of one against failure cycles from tests. This also suggests that inelastic analysis with K' of one is a good benchmark to compare against and could be treated as actual failure cycles for analytical solutions from the sample problems.

The primary limit check used the time greater than the corresponding to failure cycles of the specimen, as input in S_{mt} curves to calculate pseudo-yield stress. Pressure was identified as the load during sustained operation and was applied to the specimen during EPP FEA. Except for two cases, all others passed the primary limit check. The two cases, P09 and P07, yielded plastic collapse. A new trial time smaller than the test-specimen failure time was selected, and optimum time was calculated for these two cases, as shown in Table 3. The cyclic load results yielding at all points across thickness of the gauge length. Thus, the ratcheting-check criteria failed for all cases.

3.2. Evaluation Against Example Problems

3.2.1. Two-Bar Model

A two-bar model geometry is selected to evaluate the Class B rules. The two cylindrical bars are in series, with a corner radius of R as shown in Figure 9. Thicknesses and lengths of the system are kept constant, and three corner radii values of 1, 0.5, and 0.25 mm are selected to simulate the increasing values of stress concentrations and subsequent elastic follow-ups. The geometric parameters are selected to induce increasing elastic-stress concentration factors. Internal volumes of tubes are subjected to constant pressure, and cyclic displacements are applied with a 600 second hold at peak displacement, with ramps up and down. Material Alloy 617 was selected as the candidate material, and its isothermal state is defined at 950°C.

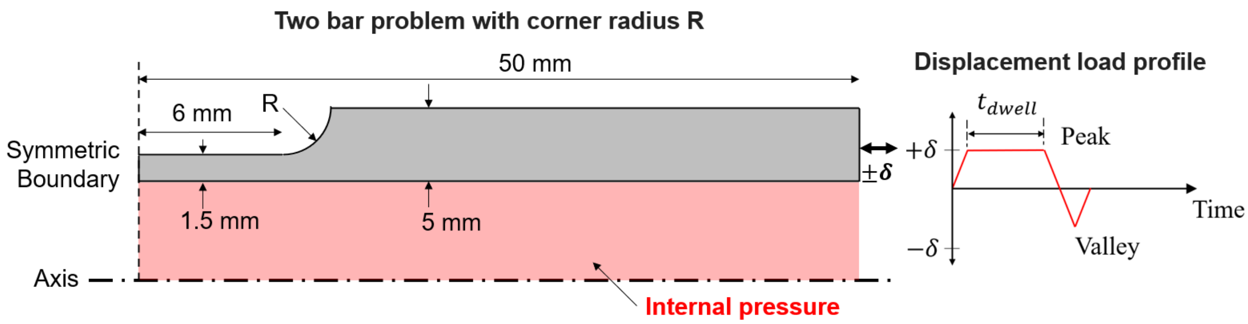

Figure 9. Schematic diagram of two-bar problem geometry and displacement-load profile.

Table 4 summarizes maximum design lives from all Class A analysis methodologies, the inelastic analysis with $K' = 1$, and from the Class B CF damage-assessment approach. Maximum design-life estimates using Class B approach result in conservative estimates compared to the Class A inelastic analysis. As discussed before, the comparison of Class A analysis methods uses assumptions and safety standards different from Class B. This report compares these methods to show the benefits of a simplified analysis approach with conservatism. The Class A elastic-analysis method is most conservative among other Class A and proposed Class B methods. Other methods in Class A, EPP analysis and inelastic analysis, are rigorous and have requirement of larger material data, time- and temperature-dependent allowable stresses, viscoplastic constitutive models, and corresponding parameters. Proposed Class B is a relatively simple DBA methodology that adapts a less-restrictive analysis approach and provides conservative estimates of design life when compared with Class A inelastic analysis and inelastic analysis with $K' = 1$, as shown in Table 4. This observation in supports Class B SSC needs to have less-restrictive design than the Class A designs.

Table 4. Maximum design-life estimate from Class B rules versus the Class A analysis methodologies.

Case ID	R (mm)	K_e	N_{max} Section III Division 5 Class A CF methodologies: Elastic	EPP	Inelastic K'=0.67	N_{max} Inelastic K'=1	N_{max} Proposed Class B rules	Ratcheting check criteria and N_{max} from ratcheting design
A	1.00	1.44	101	705	730	5292	282	Passed, 50
B	0.50	1.71	34	294	389	3198	183	Passed, 23
C	0.25	2.64	4	88	154	1529	99	Passed, 6

The equivalent stress histories at the center of the gauge length from inelastic analysis using viscoplastic model are compared against constructed stress histories calculated from maximum stress intensity, ISSCs and elastic follow-up for each case up to 10 cycles in Figure 10. The viscoplastic model captures complex material response, where stress reset is not observed for all cases when cyclic load is reloaded. Thus, stress intensities continue to relax with each cycle. In Class B stress-history calculations, stress relaxation along the elastic follow-up line on the ISSCs space is calculated for one cycle. This stress-relaxation history is used for each cycle to calculate total creep-damage fraction, resulting in a conservative creep-damage estimate relative to the inelastic-analysis approach.

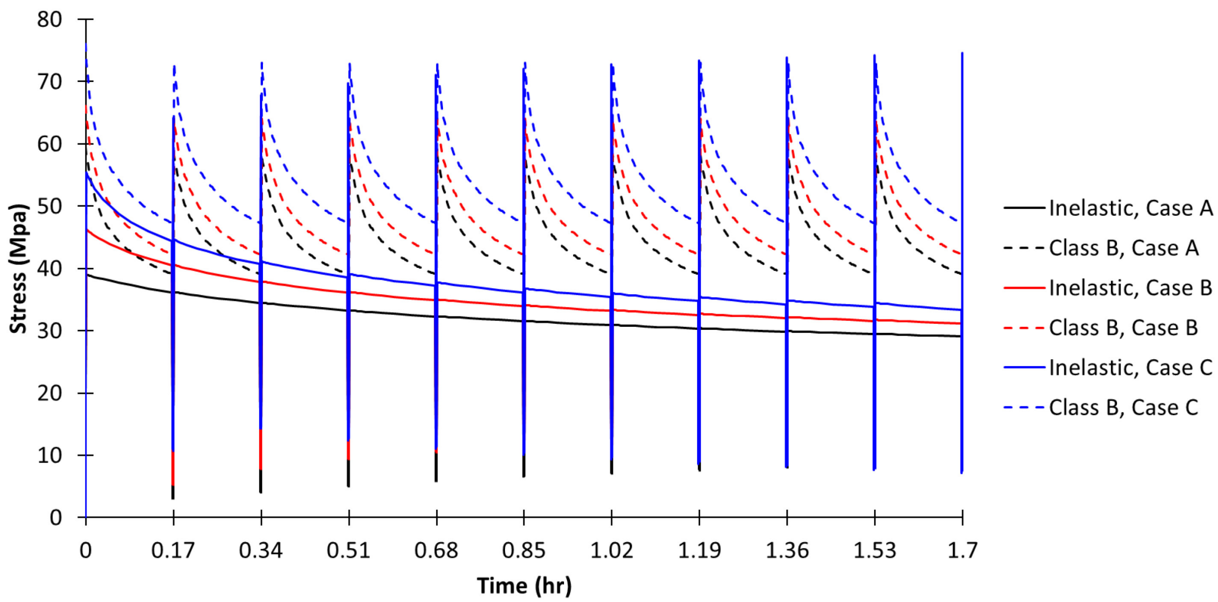

Figure 10. Comparison of equivalent stress histories from the inelastic analyses with viscoplastic model against stress-relaxation histories constructed from ISSCs and elastic follow-up for three cases.

The primary limit-check procedure used detailed geometry, with pressure as load during sustained operation. The pseudo-yield stress was calculated at a trial time of 100 hours. All three cases satisfied the primary limit check at 100 hours, meaning no plastic collapse is reached until the maximum design lives obtained from CF damage assessment. The ratcheting check started with pseudo-yield stresses at trial time. Plastic collapse was observed for the pseudo-yield stress selected at a trial time of 100 hours. Thus, an iterative procedure was used where a new trial time is selected to calculate new pseudo-yield stresses and EPP FEA was performed until no plastic collapse or ratcheting is observed at all points. The final trial time for which no ratcheting was observed is used to calculate the maximum design life, as shown in Table 4. Class A EPP strain limit evaluation per N-861 Code Case was not used for comparison. Class A EPP uses pseudo-yield stress at total strain smaller than 0.01. Class B adopts pseudo-yield stresses at 0.01 inelastic strain, suggesting Class B pseudo-yield stresses will always be greater than the Class A EPP strain limit approach. Thus, design-life estimates from Class A EPP strain-limit evaluation will be more conservative compared to the proposed Class B ratcheting-check methodology.

3.2.2. Flat Head Vessel (FHV)

Flat head vessel geometry is selected with a knuckle, modeled with a corner radius of 6.35 mm (0.25 inch) as shown in Figure 11. The stress-concentration factor at knuckle, which is calculated from the ratio total stress to the linearized stress, is 1.46. The temperature on the inside dimensions (ID) governs the load cycles and assumes the temperature profile shown in solid red color. Temperature history on outside dimensions (OD) are depicted by dashed blue lines. A component is under isothermal state during dwell time of 1000 hours. At any given time, the temperature across the thickness is assumed to be linear, and the temperature gradient across thickness, dT, is shown by a solid black line. Temperature is ramped from 500 to 700°C in 10 hours. The temperature gradient during a transient is 10°C and during the steady-state dwell time is zero. Internal pressure of 0.1 MPa is applied on ID. Stainless steel 316H is selected as candidate material.

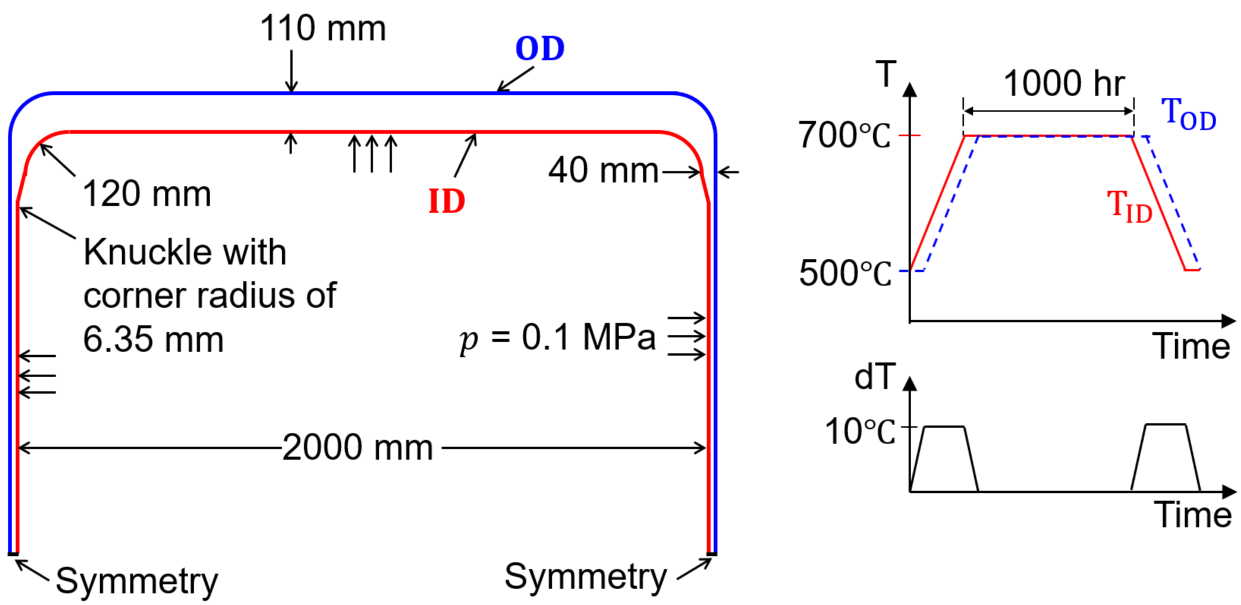

Figure 11. Flat head vessel geometry with temperature history profiles.

The temperature cycle is applied, and results from inelastic analysis were used to calculate the maximum design life. The design lives from Class A inelastic and inelastic with $K' = 1$ analyses are compared in Table 5. The stress-relaxation history used primary and secondary creep rates of Class A-material model. The predicted design life from Class B is conservative compared to the CF inelastic with $K' = 1$ method. The primary limit check used the pseudo-yield stress at 300,000 hours design life. Primary limit-check criteria passed for 300,000 hours. Pseudo-yield stress for the ratcheting check with a trial time of 300,000 hours is calculated and used in EPP FEA. The ratcheting check passed for 300,000 hours.

Table 5. Maximum design-life estimate from Class B methodology versus the Class A inelastic and inelastic analyses with K'=1 for a flat head vessel.

N_{max} Inelastic CF K'=0.67	N_{max} inelastic CF K'=1	N_{max} Class B CF rules	Primary limit check	Ratcheting check
69	407	7	Passed at 300,000 hr	Passed at 300,000 hr

4. CLASS B MATERIALS

4.1. Data Needs for Class B Code Case

The detailed material needs and potential sources of available material data for candidate Class B materials are presented. These data needs will be used as a baseline to identify the candidate-material data to develop new material properties for the Class B code case.

1. Base metal mechanical properties – This covers all mechanical properties of the base metal, including all allowable stresses, ISSCs, and fatigue-design curves. To support this development, the following information on materials is needed.
   a. Temperature-dependent allowable stresses: Yield and tensile strength over the full temperature range and trend lines for time-independent allowable stress values.
   b. Time- and temperature-dependent allowable stresses: Minimum and average creep-rupture strength and minimum creep rate for time-dependent allowable stress values. This step requires data-extrapolation procedures. Goal of the Class B case is to minimize requirement and use limited time-dependent data to develop design curves up to 500,000 hours of design life. To support design-curve development, an appropriate data-extrapolation method is needed.
      i. For Class A materials, use the available database with a standard extrapolation procedure used for Class A materials.
      ii. For candidate Class B materials and materials under Table 1A and B, use the available database with a variable-confidence index, as presented in the previous work [4].

      Material information under Tables 1A and B may not be sufficient for all materials. In that case, FFS-1, Annex 10B, "Material Data for Creep Analysis," which has equations based on Omega method for minimum and average creep-rupture strength, is proposed.
   c. Damage-envelope compatibility check: A representative CF test, similar to the fatigue acceptance test in HBB-2800, is proposed to verify the compatibility with Class B assumption for the D diagram in Table 1A and B materials.
   d. Fatigue curves: For Class A materials, use the fatigue design curves in Figures HBB-T-1420. For Table 1A and B materials, Annex 3-F, Design Fatigue Curves, in Section VIII, Div 2 provides low-temperature data for some materials. FFS-1, Annex 10B, Material Data for Creep Analysis, also has fatigue curves with references for some classes of materials. For materials with similar

chemistry, a spot-check fatigue test at several temperatures may be used to define and refine the assumed design factor.

e. Aging factors: For Class A materials, use provided aging factors in HBB as is. For Table 1A and B materials, some aging factors are provided in Table HCB-II-2000-5. For materials not specified, assign conservative factors based on broad categorization.

f. Weld-strength reduction factors: Use Class A information as is for corresponding materials. For Table 1 A and B materials, some factors are provided in Table HCB-II-2000-5. Section I and B31.1 provide factors for some materials. For materials not specified, assign conservative factors based on broad categorizations augmented with short-term creep-rupture data. This step would require literature review and to be determined by additional tests on candidate materials.

g. Negligible creep criteria: This is out of scope for initial code case development.

2. Bolting – Bolting design is referenced to Section III, Appendix XI, wherein cyclic loading and time-dependent loading are not specified.
3. Buckling – Buckling charts are provided in Section II, Part D for most materials, but for temperatures and short-term loading where creep is not an issue. There are charts for some materials providing temperature limits for the use of the time-independent buckling charts. This is part of a larger issue, and it is suggested that it not be pursued further for this code case.
4. Physical properties – Non-mandatory temperature-dependent values are provided for comprehensive set of materials. No further tabulation is suggested.

4.2. Candidate Materials

Previous work has identified the potential candidate materials to be included in Class B code case [4]. A summary list of candidate materials is presented in Table 6. Among these materials, Alloy 625 will be focused in the next fiscal year to develop the allowable stresses and design curves for the Class B code case.

Table 6. Initial candidate materials being incorporated in the new Class B Code Case.

Material type	Required material tests
Austenitic stainless steels	304H, 316H, Alloy 800H, Alloy 709, 316L
Martensitic grades	Grade 22, Grade 91 Grade 22 (N&T)
Nickel alloys	Alloy 617, Alloy 625

5. SUMMARY

The overview of Class B code case is presented showing adopted steps and a proposed methodology to address the current gaps in the existing Class B rules in HCB Section III, Division 5. The proposed methodology is evaluated against test failure data and example problems. The conservatism of proposed rules against anticipated failure modes at elevated temperatures were assessed. Proposed Class B methodology uses an elastic follow-up governed by the stress-concentration-factor to calculate the CF damage fractions. The Class B CF methodology was conservative compared to failure cycles.

Full inelastic analysis with $K' = 1$ was used in this study as a candidate for comparison. The full inelastic analysis method uses detailed geometry, with a viscoplastic material model, to capture complex realistic material response. Using $K' = 1$ results to minimize the conservatism and to best estimate failure cycles. For sample problems, proposed Class B method was compared against the inelastic with $K' = 1$. The DBA CF damage-assessment approach is conservative.

The ratcheting-check procedure is less restrictive than the Class A strain limit and ratcheting check. Class B uses pseudo-yield stresses at 0.01 plastic strain. These stresses are higher than stresses at total strain, less than 0.01. Hence, the proposed method allows use of higher yield stresses for EPP FEA. This relieves the conservatism in design for Class B SCCs.

The primary load limit check uses pseudo-yield stresses. These allowable stresses bound the material response to time-dependent material properties, such as stress-to-rupture and stress-to-reach-1% inelastic strain. This check is a good screening criterion to assess the component against rupture for sustained operational loads.

A major objective for the new Case B code case is to enable a wider selection of materials than is currently included in Class A while incorporating some of the features of Class A such as explicit consideration of design life and evaluation of cyclic service. The challenge to overcome is the extensive and long duration testing required to qualify materials for Class A construction. Because the safety requirements are less critical for Class B as compared to Class A, methodologies have been developed and approximate approaches have been identified. These approximate approaches address the time dependent and cyclic failure modes with less rigor than Class A. This enables the addition of new materials without sacrificing evaluation of time dependent and cyclic failure modes. Material data needs are listed in the report. Using this list, potential material databases will be obtained, and materials with the greatest information available will be added in the Class B code case.

6. REFERENCES

1. ASME International. 2023. "Section III, Rules for Construction of Nuclear Facility Components, Division 5, High Temperature Reactors." in ASME Boiler and Pressure Vessel Code: An International Code. New York, NY.
2. NRC. 2021. "Acceptability of ASME Code, Section III, Division 5, High Temperature Reactors." Draft Regulatory Guide DG-1380, Nuclear Regulatory Commission, Rockville, MD.
3. ASME International. 2023. "Section II, Materials Properties," in ASME Boiler and Pressure Vessel Code: An International Code." New York, NY.
4. Sham, T. -L., Y. Wang, and H. P. Mahajan. 2022. "Initial Development of Variable Design Lifetimes and Creep-Fatigue Evaluations for ASME Section III, Division 5, Class B Code Rules." INL/RPT-22-69139, Rev 0, Idaho National Laboratory, Idaho Falls, ID.
5. Mahajan, H. P., et al. 2023. "FY23 Status Report on the Development of New ASME Section III, Division 5 Class B Rules." INL/RPT-23-74748, Idaho National Laboratory, Idaho Falls, ID.
6. ASME International. 2023. "Code Cases, Boilers and Pressure Vessels." in ASME Boiler and Pressure Vessel Code: An International Code. New York, NY.
7. ASME International. 2021. "Section III, Rules for Construction of Nuclear Facility Components, Appendices," in ASME Boiler and Pressure Vessel Code: An International Code. New York, NY.
8. Messner, M. C., and T. -L. Sham. 2021. "Reference constitutive model for Alloy 617 and 316H stainless steel for use with the ASME Division 5 design by inelastic analysis rules." ANL-ART-225, Argonne National Laboratory, Lemont, IL. https://doi.org/10.2172/1818970.
9. Wang, Y. et al. 2021. "Evaluation of Primary-load Effects on Creep-Fatigue Life of Alloy 617 Using Simplified Model Test Method." In proceedings of the ASME 2021 Pressure Vessels and Piping Conference, Virtual, July 13–15. https://doi.org/10.1115/PVP2021-61658.
10. Wang, Y., et al. 2020. "Report on FY2020 Test Results in Support of the Development of EPP Plus SMT Design Method." ORNL/TM-2020/1620, Oak Ridge National Laboratory, Oak Ridge, TN. https://doi.org/10.2172/1659599.

11. Wang, Y., R. I. Jetter, and T. L. Sham. 2017. "Pressurized Creep-Fatigue Testing of Alloy 617 Using Simplified Model Test Method." In proceedings of the ASME 2017 Pressure Vessels and Piping Conference, Waikoloa, HI, July 16–20. https://doi.org/10.1115/PVP2017-65457.

12. Wang, Y., et al. 2019. "Report on FY19 Testing in Support of Integrated EPP-SMT Design Methods Development." ORNL/TM-2019/1224, Oak Ridge National Laboratory, Oak Ridge, TN. https://doi.org/10.2172/1564187.

13. Wang, Y., R. I. Jetter, and T. L. Sham. July 2019. "Effect of Internal Pressurization on the Creep-Fatigue Performance of Alloy 617 Based on Simplified Model Test Method." In proceedings of the ASME 2019 Pressure Vessels and Piping Conference, San Antonio, TX, July 14–19. https://doi.org/10.1115/PVP2019-93650.